

Electrostatic vibration energy harvester with 2.4-GHz Cockcroft-Walton rectenna start-up

Hakim Takhedmit, Zied Saddi, Armine Karami, Philippe Basset, Laurent Cirio

▶ To cite this version:

Hakim Takhedmit, Zied Saddi, Armine Karami, Philippe Basset, Laurent Cirio. Electrostatic vibration energy harvester with 2.4-GHz Cockcroft–Walton rectenna start-up. Comptes Rendus. Physique, 2017, 18 (2), pp.98-106. 10.1016/j.crhy.2016.12.001. hal-01434988

HAL Id: hal-01434988

https://hal.sorbonne-universite.fr/hal-01434988v1

Submitted on 13 Jan 2017

HAL is a multi-disciplinary open access archive for the deposit and dissemination of scientific research documents, whether they are published or not. The documents may come from teaching and research institutions in France or abroad, or from public or private research centers. L'archive ouverte pluridisciplinaire **HAL**, est destinée au dépôt et à la diffusion de documents scientifiques de niveau recherche, publiés ou non, émanant des établissements d'enseignement et de recherche français ou étrangers, des laboratoires publics ou privés.



C. R. Physique ••• (••••) •••-••

FISEVIER

Contents lists available at ScienceDirect

Comptes Rendus Physique

www.sciencedirect.com



Energy and radiosciences / Énergie et radiosciences

Electrostatic vibration energy harvester with 2.4-GHz Cockcroft–Walton rectenna start-up

Dispositif de récupération d'énergie vibratoire par transduction électrostatique, pré-chargé par une rectenna Cockcroft–Walton à 2,4 GHz

Hakim Takhedmit ^{a,*}, Zied Saddi ^a, Armine Karami ^b, Philippe Basset ^a, Laurent Cirio ^a

ARTICLE INFO

Article history:
Available online xxxx

Keywords:
Rectenna
Cockcroft-Walton rectifier
Energy harvesting
Electrostatic transduction
Bennet's doubler

Mots-clés: Rectenna Circuit de rectification Cockcroft-Walton Récupération d'énergie Transduction électrostatique Doubleur de tension de Bennet

ARSTRACT

In this paper, we propose the design, fabrication and experiments of a macro-scale electrostatic vibration energy harvester (e-VEH), pre-charged wirelessly for the first time with a 2.4-GHz Cockcroft–Walton rectenna. The rectenna is designed and optimized to operate at low power densities and provide high voltage levels: 0.5 V at 0.76 μ W/cm² and 1 V at 1.53 μ W/cm². The e-VEH uses a Bennet doubler as a conditioning circuit. Experiments show a 23-V voltage across the transducer terminal, when the harvester is excited at 25 Hz by 1.5 g of external acceleration. An accumulated energy of 275 μ J and a maximum available power of 0.4 μ W are achieved.

© 2016 Académie des sciences. Published by Elsevier Masson SAS. This is an open access article under the CC BY-NC-ND license

(http://creativecommons.org/licenses/by-nc-nd/4.0/).

RÉSUMÉ

Cet article propose la conception, la réalisation et les mesures d'un transducteur électrostatique, à base d'une capacité macroscopique, pré-chargé par une rectenna de type Cockcroft–Walton à 2,4 GHz. La rectenna est conçue et optimisée pour fonctionner à des niveaux de puissance faibles et fournir des tensions élevées : 0,5 V à 0,76 μ W/cm² et 1 V à 1,53 μ W/cm². Le transducteur électrostatique utilise le circuit de conditionnement de Bennet. Les mesures du système complet montrent des tensions supérieures à 23 V aux bornes du transducteur, lorsqu'il est excité à 25 Hz et avec une accélération externe de 1,5 g. Une énergie cumulée de 275 μ J et une puissance disponible de 0,4 μ W ont pu être obtenues.

© 2016 Académie des sciences. Published by Elsevier Masson SAS. This is an open access article under the CC BY-NC-ND license

(http://creative commons.org/licenses/by-nc-nd/4.0/).

E-mail address: hakim.takhedmit@u-pem.fr (H. Takhedmit).

http://dx.doi.org/10.1016/j.crhy.2016.12.001

1631-0705/© 2016 Académie des sciences. Published by Elsevier Masson SAS. This is an open access article under the CC BY-NC-ND license (http://creativecommons.org/licenses/by-nc-nd/4.0/).

^a Université Paris-Est, ESYCOM (EA 2552), UPEM, ESIEE-Paris, CNAM, 77454 Marne-la-Vallée, France

^b Laboratoire d'informatique de Paris 6 (LIP6), Université Paris 6, Paris 75005, France

^{*} Corresponding author.

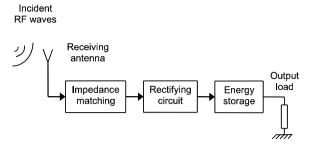


Fig. 1. Block diagram of an RF energy harvester.

1. Introduction

Advances in wireless communications and low-consumption electronics in recent decades have contributed to the emergence of sensors and connected objects in different fields. An exponential growth of the number of devices is expected with the advent of the Machine-to-Machine (M2M) and the Internet of Things (IoT). The energy autonomy of such devices constitutes one of the main obstacles before reaching full mobility. Instead of traditional batteries that require periodic replacement or recharging and raise recycling issues, energy harvesting, consisting in converting the energy of ambient sources such as electromagnetic waves, vibrations, thermal, solar and wind into electrical energy, became a potentially promising solution. From these ambient sources, electromagnetic waves and mechanical vibrations are of particular relevance due to their availability. Vibration harvesters are based on the transduction mechanism, and they are typically of three kinds: electromagnetic, piezoelectric and electrostatic [1-5]. In electrostatic-vibration energy harvesters (e-VEHs), mechanical energy is converted into electricity by a mechanical attraction force due to charged variable capacitor plates. This force opposes the motion of the mobile plate. The generated power from mechanical to electrical conversion is proportional to the square of the accumulated quantity of charge in the capacitor. Therefore, an external source providing sufficient voltage is necessary to convert vibrations into electricity in a sufficient manner. One solution consists in using an electret layer [6,7]. Another solution consists in using a transducer pre-charge containing a power source and a conditioning circuit that generates the bias voltage itself and then creates a force between the two plates of the variable capacitor [8–14]. In this paper, we propose the use of an RF energy harvester, commonly called rectenna [15-23], to pre-charge an e-VEH device. Several configurations of rectennae are reported in the literature, the single series [16-18] and shunt [16-19] are the most used. However, such topologies deliver small DC voltages. Indeed, for higher output, the voltage doubler [16,20,21], the Greinacher topology [22] and the voltage multiplier [23] are further appropriate.

Usually, when designing rectennas, the main issue consists in maximizing the electrical power delivered to the load or the RF-to-dc conversion efficiency [24,25]. A new and efficient dual-diode rectenna was reported in [24]. A global efficiency higher than 80% and a dc output voltage of 2.6 V over a 1050- Ω resistive load have been achieved at a power density of 0.22 mW/cm² ($E \sim 29$ V/m). A compact and efficient 2.45-GHz rectenna was presented in [25], where a circularly polarized shorted ring-slot antenna was used. The reported rectenna exhibits a maximum efficiency of 69% and an output dc voltage of 1.1 V at a low power density of 20 μ W/cm² (E = 8.7 V/m).

This paper describes the design, fabrication and experiments of an e-VEH, with a Bennet doubler as the conditioning circuit, pre-charged by a rectenna circuit at 2.4 GHz. The outline is as follows. Section 2 presents the design and experiments of the Cockcroft–Walton rectenna. The fabrication and operation of the mechanical transducer, including the Bennet doubler, is reported in Section 3. Further, in Section 4, the experimental results of the full circuit are presented and discussed. Finally, section 5 concludes the paper.

2. Cockcroft-Walton rectenna at 2.4 GHz

The bloc diagram of an RF power harvester is illustrated in Fig. 1. It contains a receiving antenna followed by an RF-to-dc rectifier and optionally an energy storage device.

A rectifier is often made up of a combination of Schottky diodes, an input RF filter, and an output bypass capacitor. The input filter, localized between the receiving antenna and the diodes, is a low-pass filter that rejects unwanted high-order harmonics created by the non-linear behavior of the diodes. It also provides impedance matching between the antenna and the rectifier [15,16].

To pre-charge the e-VEH, high output voltage is suitable. The single series, the single shunt or even the voltage doubler were shown to be insufficient. Other topologies, less conventional, should be used. The Cockcroft–Walton voltage multiplier with several cascaded stages proves to be an efficient solution [26,27]. This section describes the study of such a circuit, from design to experiments.

Fig. 2. Voltage multiplier scheme (a); one stage multiplier (b).

(b)

(a)

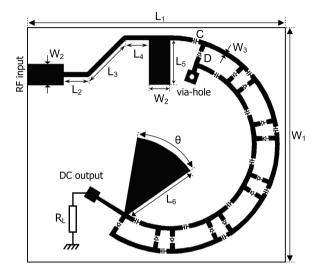


Fig. 3. Geometry of the rectifier: $L_1 = 45$, $L_2 = 4$, $L_3 = 8.4$, $L_4 = 4$, $L_5 = 7.3$, $L_6 = 12.5$, $W_1 = 46$, $W_2 = 3.5$, $W_3 = 0.8$, $\theta = 45^{\circ}$ (dimensions are in millimeters).

2.1. Voltage multiplier design

The voltage multiplier scheme is shown in Fig. 2a. It contains several identical cascaded stages; each stage contains two Skyworks SMS 7630 Schottky diodes (D_1 and D_2) [28] and two equal capacitors (C_1 and C_2) as illustrated in Fig. 2b.

The output DC voltage depends on the capacitors C_1 and C_2 and even more on the number of stages. It increases when the number of stages increases. However, for an RF power level, there is a tradeoff between the number of stages and losses. Indeed, when losses (substrate, parasitic components, electromagnetic couplings...), become important the voltage gain becomes insignificant.

A microstrip Cockcroft–Walton voltage multiplier, operating at 2.4 GHz, is proposed (Fig. 3). It is designed and optimized, under ADS (Advanced Design System) software, by using a global analysis technique [29]. The simulations were achieved by coupling a momentum electromagnetic simulator and Harmonic Balance (HB). The circuit contains six cascaded stages and is fed by a microstrip line ($Z_c = 50~\Omega$). The circuit is etched on Arlon 25N substrate ($\varepsilon_r = 3.4$, thickness = 1.524 mm, $\tan \delta = 0.0025$). Series capacitors ($C = 68~\mathrm{pF}$) were properly chosen and modeled, by taking into account their parasitic effects. The output load R_L is very large: it is set at 100 M Ω . A quarter wavelength radial stub (L_6 , θ) isolates the output load from RF incident power. To achieve an impedance matching between the RF source (or receiving antenna) and the rectifier, an open stub (L_5 , W_2) associated with a quarter wavelength transformer ($L_2 + L_3 + L_4$, W_3) was calculated and used. The circular topology of the design and the arrangement of the different components are carefully chosen to decrease the dimensions of the circuit.

2.2. Experimental characterization

The circuit was fabricated and measured. Fig. 4 shows the simulated and measured output dc voltage against frequency, from 0.5 to 4 GHz, at -15 dB m. Good agreement can be observed between theoretical and experimental results. At 2.4 GHz, the measured dc voltage is 0.85 V, and that achieved by ADS simulation is 1.05 V.

Fig. 5 shows a comparison between the simulated and measured curves of dc voltage, as a function of the input RF power from -25 to -5 dBm, at 2.4 GHz. Maximum output dc voltages of 3.16 and 3.36 V have been obtained by ADS simulation and experiment, respectively.

3

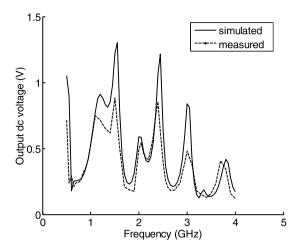


Fig. 4. Output dc voltage vs. frequency.

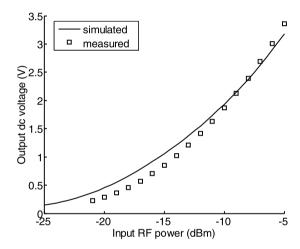


Fig. 5. Output dc voltage vs. input RF power.

A microstrip patch antenna, operating at 2.4 GHz, was designed and associated with the rectifier. It presents an input return loss of 19 dB and a gain of 4 dBi. The full rectenna was characterized inside an anechoic chamber. The measurement setup contains an RF source and a 12-dBi gain transmitting horn antenna. The device under test is placed in the far field region at a distance of 1.5 m from the horn antenna. Fig. 6 shows the dc output voltage against power density from 0 to $10 \,\mu\text{W/cm}^2$. Our results show that when power density increases, dc voltage increases. However, for higher power densities, the output voltage is limited by the reverse breakdown voltage of the diodes. Measured dc voltages of 1, 2 and 3 V are obtained at 1.53 $\mu\text{W/cm}^2$ ($E=2.4 \,\text{V/m}$), 3.5 $\mu\text{W/cm}^2$ ($E=3.63 \,\text{V/m}$) and 8 $\mu\text{W/cm}^2$ ($E=5.5 \,\text{V/m}$) power densities (electric field strength), respectively.

Fig. 7 represents the measured voltage evolution, over a capacitive load of 1 mF, for different power densities: 1, 3 and $10 \, \mu \text{W/cm}^2$. The results show that the capacitor takes less than 5 min to charge and then stores energy of about 281 μ J at $1 \, \mu \text{W/cm}^2$, $1620 \, \mu$ J at $3 \, \mu \text{W/cm}^2$ and $5445 \, \mu$ J at $10 \, \mu \text{W/cm}^2$.

3. Electrostatic vibration energy harvester

3.1. Conditioning circuit

Most conditioning circuits reported in the literature require inductive elements and switches [8–12] to generate a high bias voltage. However, inductive elements are not compatible with a batch manufacturing process and switches require additional power-consumption-control circuits. Recently issued, a conditioning circuit based on the Bennet doubler generated high bias voltage without using any switch or inductor [13,14]. Its operation has been demonstrated with a macro-scale variable differential capacitor, whose variation was induced by an external motor. Moreover, authors in [30] present the study of a monophase (single capacitor) MEMS e-VEH using such a kind of conditioning circuit. Fig. 8 shows Bennet's dou-

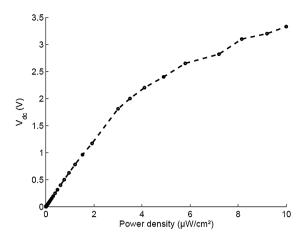


Fig. 6. Measured dc voltage vs. power density ($R_L = 100 \text{ M}\Omega$).

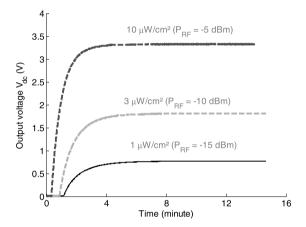


Fig. 7. Voltage waveform over capacitive load (C = 1 mF).

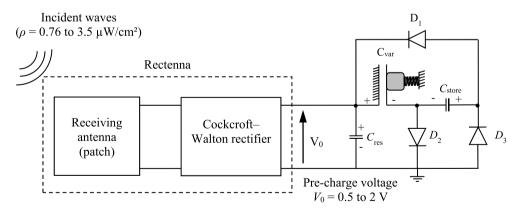


Fig. 8. Bennet's doubler conditioning circuit.

bler circuit, it contains three capacitors, the variable capacitor C_{var} , $C_{\text{res}} = 1 \, \mu\text{F}$, and $C_{\text{store}} = 47 \, \text{nF}$, and three diodes D_1 , D_2 and D_3 (JPAD5). The initial pre-charge V_0 applied to C_{res} is supplied by the rectenna presented in the previous section. The operation of Bennet's doubler is described in [30].

3.2. Description of the structure

The schematic drawing of the e-VEH prototype is shown in Fig. 9.

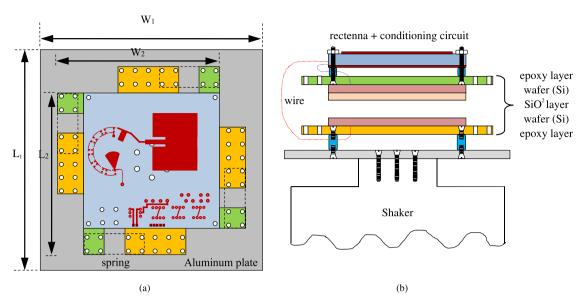


Fig. 9. Geometry of the e-VEH: $L_1 = W_1 = 150$, $L_2 = 119$, $W_2 = 100$ (dimensions are in mm). Top view (a) and profile view (b).

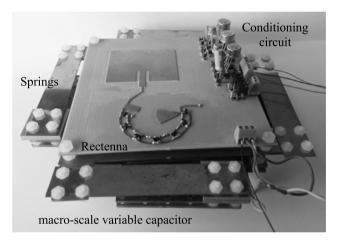


Fig. 10. Photograph of the prototype showing the Cockcroft-Walton rectenna, the conditioning circuit and the macro-scale variable capacitor.

The device includes a macro-scale variable capacitor and a Bennet doubler conditioning circuit. The top view (Fig. 9a) shows the rectenna and the conditioning circuit on the same substrate, which is linked to the mobile plate of the variable capacitor with four Teflon bolts (Fig. 9b). The macro-scale variable capacitor is made by two circular doped silicon wafers 100 mm in diameter and 0.5 mm in thickness, pasted on a square epoxy board 1.5 mm in thickness. The wafer of the mobile plate is provided with a 50-µm-thick SiO₂ insulating layer to prevent short circuits with the second wafer. The second plate of the variable capacitor is fixed to a shaker. Four flat metal springs, 60 mm in length and 15 mm in width, are used to link the two plates of the variable capacitor, one on each side of the epoxy layer. These springs were dimensioned so that the mobile plate of the capacitor remains parallel to the fixed one when it moves. Each end of a spring is fixed to the PCB layers using four nylon bolts.

4. Experiments of the e-VEH system

The photograph of the prototype is depicted in Fig. 10. The experiments were carried out using the macro-scale resonant variable capacitor described in the previous section. The resonance frequency was 25 Hz. The measured unbiased transducer capacitance variation of 1.5 g amplitude at 25 Hz frequency was: $C_{\text{max}}/C_{\text{min}} = 250 \text{ pF}/40 \text{ pF}$ ($\eta = 6.25$).

Fig. 11 shows the schematic diagram of the experimental setup. The e-VEH prototype is mounted on a shaker (Bruel & Kjaer type 7541) and placed in an anechoic chamber at a distance R = 1.5 m from a transmitting horn antenna, where the far-field condition is satisfied. An accelerometer, adhered to the shaker, is used to control and then regulate the acceleration. The experiment was carried using external vibrations at 25 Hz with an acceleration amplitude of $1.5 \, \mathrm{g}$.

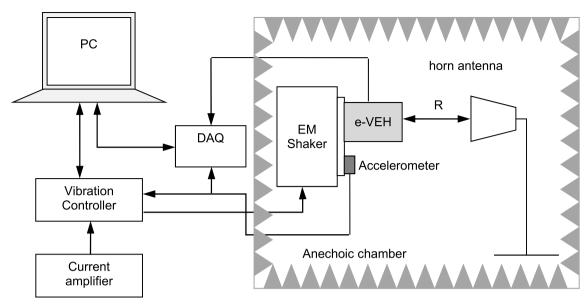


Fig. 11. Schematic diagram of the experimental setup.

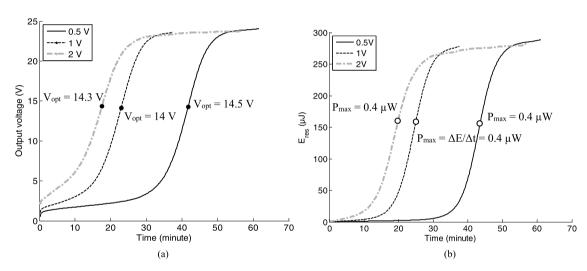


Fig. 12. Measured evolution of voltage across Cres (a) and accumulated energy on Cres (b) for several bias voltages of 0.5, 1 and 2 V, with 25 Hz/1.5g external vibrations.

The measured voltage evolution across C_{res} at several pre-charge voltages is shown in Fig. 12a. The output voltage progressively increases up to 23 V, where saturation occurs. This voltage increase across C_{res} corresponds to the accumulated energy. The saturation of the voltage across C_{res} is due to the spring-softening effect induced by electromechanical coupling [30]. Indeed, the frequency corresponding to the maximum displacement of the harvester's movable electrode decreases progressively when the self-biasing provided by the conditioning circuit increases [31]. At some point, this frequency of maximum displacement is too far from the frequency of the mechanical excitation, and the power gain due to the bias increase is balanced by a smaller transducer capacitance variation. For different pre-charge voltages, the output voltage across C_{res} tends towards the same value. However, the time required to achieve saturation decreases when bias voltage increases. The optimal voltage, which is defined as the maximum gradient of voltage $\Delta V/\Delta t$, is calculated for different values of the pre-charge voltage. The values of $V_{\rm opt}$ and the required time to reach it are summarized in Table 1.

The energy accumulated in C_{res} , for different values of the pre-charge voltage (0.5, 1, and 2 V), is plotted in Fig. 12b. Energy increases against time and reaches more than 275 µJ in a few tens of minutes. The maximum available power, defined as the gradient of energy $\Delta E/\Delta t$, is calculated for different curves. When the bias voltage increases, the e-VEH needs less time to reach the maximum available power of $0.4 \mu W$. The results are summarized in Table 1.

The accumulated energy is mainly provided by the mechanical transducer. Indeed, the rectenna provides only 0.125, 0.5 and 2 µJ for pre-charge voltages of 0.5, 1 and 2 V, respectively.

Table 1 Optimal voltage and maximum available power for different pre-charge voltages, with 25 Hz/1.5 g external vibrations.

Bias voltage (V)	Optimal voltage (V)	Maximum available power (μW)	Required time (min)
0.5	14.5	0.4	43
1	14	0.4	24
2	14.3	0.4	19

5. Conclusion

This paper presents the first experiments relating to an electrostatic-vibration energy-harvester start-up using RF waves. The RF harvester consists of a Cockcroft–Walton rectenna at 2.4 GHz. The circuit was fabricated and validated. It provides 0.5 V at $0.76~\mu\text{W}/\text{cm}^2$ and 2 V at $3.5~\mu\text{W}/\text{cm}^2$. The Bennett doubler is used as the conditioning circuit. It does not need any inductive element or switch. Experiments show a 23-V voltage across the transducer terminal, when the harvester is excited at 25 Hz by 1.5~g of external acceleration. An accumulated energy of 275 μ J and a maximum power of $0.4~\mu\text{W}$ are available for the load.

References

- [1] P. Glynne-Jones, M.J. Tudor, S.P. Beeby, N.M. White, An electromagnetic, vibration-powered generator for intelligent sensor systems, Sens. Actuators A, Phys. 110 (1–3) (2004) 344–349.
- [2] X. Cao, W.-J. Chiang, Y.-C. King, Y.-K. Lee, Electromagnetic energy harvesting circuit with feedforward and feedback DC-DC PWM boost converter for vibration power generator system, IEEE Trans. Power Electron. 22 (2) (2007) 679–685.
- [3] L-C.J. Blystad, E. Halvorsen, S. Husa, Piezoelectric MEMS energy harvesting systems driven by harmonic and random vibrations, IEEE Trans. Ultrason. Ferroelectr. Freq. Control 57 (4) (2010) 908–919.
- [4] P.D. Mitcheson, E.M. Yeatman, G.K. Rao, A.S. Holmes, T.C. Green, Energy harvesting from human and machine motion for wireless electronic devices, Proc. IEEE 96 (9) (2008) 1457–1486.
- [5] Y. Lu, F. Cottone, S. Boisseau, F. Marty, D. Galayko, P. Basset, A nonlinear MEMS electrostatic kinetic energy harvester for human-powered biomedical devices, Appl. Phys. Lett. 107 (2015) 253902.
- [6] Y. Suzuki, D. Miki, M. Edamoto, M. Honzumi, A MEMS electret generator with electrostatic levitation for vibration-driven energy harvesting applications, J. Micromech. Microeng. 20 (10) (2010) 104002 [8 pp.].
- [7] Y. Lu, E. O'Riordan, F. Cottone, S. Boisseau, D. Galayko, E. Blokhina, F. Marty, P. Basset, A batch-fabricated electret-biased wideband MEMS vibration energy harvester with frequency-up conversion behavior powering a UHF wireless sensor node, J. Micromech. Microeng. 26 (12) (2016) 124004, http://dx.doi.org/10.1088/0960-1317/26/12/124004.
- [8] A. Dudka, P. Basset, F. Cottone, E. Blokhina, D. Galayko, Wideband electrostatic vibration energy harvester (e-veh) having a low start-up voltage employing a high-voltage integrated interface, J. Phys. Conf. Ser. 476 (2013) [1–5].
- [9] A. Kempitiya, D. Borca-Tasciuc, M.M. Hella, Low-power ASIC for microwatt electrostatic energy harvesters, IEEE Trans. Ind. Electron. 60 (12) (2013) 5639–5647.
- [10] S. Meninger, J. Mur-Miranda, R. Amirtharajah, A. Chandrakasan, J. Lang, Vibration-to-electric energy conversion, IEEE Trans. Very Large Scale Integr. (VLSI) Syst. 9 (1) (2001) 64–76.
- [11] E.O. Torres, G.A. Rincon-Mora, Electrostatic energy-harvesting and battery-charging CMOS system prototype, IEEE Trans. Circuits Syst. I, Regul. Pap. 56 (9) (2009) 1938–1948.
- [12] S. Roundy, P.K. Wright, J. Rabaey, A study of low level vibrations as a power source for wireless sensor nodes, Comput. Commun. 26 (11) (2003) 1131–1144;
- B.C. Yen, J.H. Lang, A variable-capacitance vibration-to-electric energy harvester, IEEE Trans. Circuits Syst. I, Regul. Pap. 53 (2) (2006) 288–295. [13] A.C.M. de Queiroz, M. Domingues, The doubler of electricity used as battery charger, IEEE Trans. Circuits Syst. II, Express Briefs 58 (12) (2011) 797–801.
- [14] V. Dragunov, V. Dorzhiev, Electrostatic vibration energy harvester with increased charging current, J. Phys. Conf. Ser. 476 (2013) 012115 [5 pp.].
- [15] Y.J. Ren, K. Chang, 5.8-GHz circularly polarized dual-diode rectenna and rectenna array for microwave power transmission, IEEE Trans. Microw. Theory Tech. 54 (4) (2006) 1495–1502.
- [16] A. Douyere, J.D. Lan Sun Luk, F. Alicalapa, High efficiency microwave rectenna circuit: modeling and design, Electron. Lett. 44 (24) (2008) 1409–1410.
- [17] J. Zbitou, M. Latrach, S. Toutain, Hybrid rectenna and monolithic integrated zero-bias microwave rectifier, IEEE Trans. Microw. Theory Tech. 54 (1) (2006) 147–152.
- [18] J.A.G. Akkermans, M.C. Van Beurden, G.J.N. Doodeman, H. Visser, Analytical models for low-power rectenna design, IEEE Antennas Wirel. Propag. Lett. 4 (2005) 187–190.
- [19] B. Strassner, K. Chang, 5.8-GHz circularly polarized rectifying antenna for wireless microwave power transmission, IEEE Trans. Microw. Theory Tech. 50 (8) (2002) 1870–1876.
- [20] J. Heikkinen, M. Kivikoski, Low-profile circularly polarized rectifying antenna for wireless power transmission at 5.8 GHz, IEEE Microw. Wirel. Compon. Lett. 14 (4) (2004) 162–164.
- [21] J. Heikkinen, M. Kivikoski, A novel dual-frequency circularly polarized rectenna, IEEE Antennas Wirel. Propag. Lett. 2 (2003) 330-333.
- [22] U. Olgun, C.C. Chen, J.L. Volakis, Design of an efficient ambient WiFi energy harvesting system, IET Microw. Antennas Propag. 6 (11) (2012) 1200-1206.
- [23] H. Takhedmit, H. Kilani, L. Cirio, P. Basset, O. Picon, Design and experiments of a 2.4-GHz voltage multiplier for RF energy harvesting, in: Proc. Power MEMS, 2012, pp. 448–451.
- [24] H. Takhedmit, L. Cirio, B. Merabet, B. Allard, F. Costa, C. Vollaire, O. Picon, Efficient 2.45 GHz rectenna design including harmonic rejecting rectifier device, Electron. Lett. 46 (12) (2010) 811–812.
- [25] H. Takhedmit, L. Cirio, S. Bellal, D. Delcroix, O. Picon, Compact and efficient 2.45 GHz circularly polarised shorted ring-slot rectenna, Electron. Lett. 48 (5) (2012) 253–254.
- [26] H. Yan, J.G. Macias Montero, A. Akhnoukh, L. de Vreede, J. Burghartz, An integration scheme for RF power harvesting, in: Proc. Proceedings of the STW Annual Workshop on Semiconductor Advances for Future Electronics and Sensors, SAFE 2005, Utrecht, The Netherlands, 17–18 November 2005, 2005, pp. 64–66.

ARTICLE IN PRESS

COMREN:3363

H. Takhedmit et al. / C. R. Physique ••• (••••) •••-••

- [27] T. Sogorb, J.V. Llario, J. Pelegri, R. Lajara, J. Alberola, Studying the feasibility of energy harvesting from broadcast RF station for WSN, in: Proc. 2008 IEEE Instrumentation and Measurement Technology Conference, 12–15 May 2008, Victoria, British Columbia, CA, 2008, pp. 1360–1363.
- [28] Datasheet surface mount mixer and detector Schottky diodes skyworks, http://www.skyworksinc.com.
- [29] H. Takhedmit, B. Merabet, L. Cirio, B. Allard, F. Costa, C. Vollaire, O. Picon, Design of a 2.45 GHz rectenna using a global analysis technique, in: Proc. 3rd European Conference on Antennas and Propagation, EuCAP 2009, 23–27 March, Berlin, Germany, 2009, pp. 2321–2325.
- [30] V. Dorzhiev, A. Karami, P. Basset, F. Marty, V. Dragunov, D. Galayko, Electret-free micromachined silicon electrostatic vibration energy harvester with the Bennet's Doubler as conditioning circuit, IEEE Electron Device Lett. 36 (2) (2015) 183–185.
- [31] P. Basset, E. Blockhina, D. Galayko, Electrostatic Kinetic Energy Harvesters, Smart Adaptive Systems on Silicon Series, Wiley/ISTE, ISBN 978-1-84821-716-4, 2016 (244 p.).

9